RESEARCH ARTICLE | MARCH 15 2012

Application of efficient algorithm for solving six-dimensional molecular Ornstein-Zernike equation

R. Ishizuka; N. Yoshida

J. Chem. Phys. 136, 114106 (2012)
https://doi.org/10.1063/1.3693623

Application of efficient algorithm for solving six-dimensional molecular Ornstein-Zernike equation

R. Ishizuka[1,a)] and N. Yoshida[2,3]
[1]*Department of Biochemistry and Molecular Biology, University of Texas Medical Branch at Galveston, Galveston, Texax 77555-1068, USA*
[2]*Department of Chemistry, Graduate School of Sciences, Kyushu University, Fukuoka 812-8581, Japan*
[3]*Institute for Advanced Study, Kyushu University, Fukuoka 812-8581, Japan*

(Received 5 December 2011; accepted 24 February 2012; published online 15 March 2012)

In this article, we propose an efficient algorithm for solving six-dimensional molecular Ornstein-Zernike (MOZ) equation. In this algorithm, the modified direct inversion in iterative subspace, which is known as the fast convergent method for solving the integral equation theory of liquids, is adopted. This method is found to be effective for the convergence of the MOZ equation with a simple initial guess. For the accurate averaging of the correlation functions over the molecular orientations, we use the Lebedev-Laikov quadrature. The appropriate number of grid points for the quadrature is decided by the analysis of the dielectric constant. We also analyze the excess chemical potential of aqueous ions and compare the results of the MOZ with those of the reference interaction site model.
 [http://dx.doi.org/10.1063/1.3693623]

I. INTRODUCTION

Molecular Ornstein-Zernike (MOZ) equation with the full hypernetted chain (HNC) approximation is a powerful method to calculate properties of liquid and solutions. After the pioneering works of Blum and Torrlella,[1–3] considerable efforts have been devoted to the establishment of numerical techniques suited to the MOZ equation.[4–7] Relatively simplified models have been applied to the studies of liquids because of the mathematical complexity and expensive computational cost of the MOZ theory. The reference interaction site model (RISM) which was proposed by Chandler and Andersen[8] is the most popular model among them. In that formalism, the six-dimensional MOZ equation is replaced by a set of one-dimensional site-site integral equations.[9] The numerical schemes for solving the RISM equation have been well established and applied to many chemical and biological problems in the past decades.[9,10] In spite of qualitative successes, some failures of the RISM have been noted. First, the RISM is known to be poor for dielectric properties of liquids, yielding essentially trivial results.[11,12] Second, the RISM is graphically unsound, which generates the unallowed graphs in its cluster expansions.[13,14] These deficiencies have been attributed to the treatment of the asymptotic behavior for the long range Coulomb interaction and neglected dielectric bridge corrections in site-site closure approximations. In contrast, since the MOZ equation handles the mutual orientations of the molecules explicitly, it can be applied to the studies of liquids without struggling with these problems.[15] Improvements of numerical methods for solving the MOZ equation are, therefore, important.

A large number of methods exist for solving the integral equations of liquids.[16,17] The simplest scheme is the Picard iteration,[18] which, however, can converge rather slowly. A widely used scheme is the Newton-Raphson (NR) algorithm combined with the Picard iteration, the so-called Gillan method.[19] Similar schemes are used also in the Labik-Malijevsky-Vonka method [20,21] or wavelet-based methods.[22–24] Although the NR method gives an essential improvement with respect to the Picard iteration, its convergence also depends on the prepared initial guess. In order to avoid divergence, the NR scheme can be started at high temperature or low density. Consequently, it requires a large number of iteration steps for obtaining the solution at ambient condition. On the other hand, direct inversion in iterative subspace (DIIS), also known as Pulay mixing,[25,26] shows the good convergence with less dependence on initial guesses. A modification of DIIS which was proposed by Kovalenko and co-workers[27] has been proven to be effective for the convergence of the RISM equation. It comprises two stage: minimization of the residual linearly approximated with last successive iterative vectors used as a current basis, and then update of the basis with minimized approximate residual by a properly scaled parameter. Although the modified direct inversion in iterative subspace (MDIIS) requires the much more expensive computational cost than the NR algorithm does, the recent developments of parallel computing scheme make it feasible not only for solving the RISM but also for the six-dimensional MOZ equation.

In this article, we apply the MDIIS method to MOZ calculations for bulk water and aqueous ion. For accurate evaluation of the rotational invariant coefficients, the Lebedev-Laikov quadrature[28] was used for integrating the molecular pair correlation function over orientations. Using this quadrature, the angular integration with spherical harmonic functions can be performed within fewer angular grid points than that of a Gauss quadrature. In our method, the rotational invariant coefficients of the long-range part of the direct correlation function was calculated from a fivefold integration of the Coulomb potential without using the

a)Electronic mail: ryo.ishizuka@gmail.com.

conventional multipole expansion,[29] which can include the effect of the overlap of molecules. An analytical expression of its coefficients in Fourier space was also obtained. We have implemented these results into the Hankel transform of the direct correlation function. Technical detail of the fivefold integration using the Lebedev-Laikov quadrature and extension of the MDIIS to the MOZ equation is given in Sec. III. In Sec. IV, we chose appropriate grid points for the Lebedev-Laikov quadrature through an analysis of the dielectric constant of ambient water. We will also compare the excess chemical potential of aqueous ions calculated from the MOZ equation with those from the RISM theory.

II. THEORY

The MOZ theory consists of simultaneously solving the Ornstein-Zernike equation,

$$\eta(\mathbf{R}_{12}, \mathbf{\Omega}_1, \mathbf{\Omega}_2) = \frac{\rho}{8\pi^2} \int\int_{-\infty}^{\infty} c(\mathbf{R}_{13}, \mathbf{\Omega}_1, \mathbf{\Omega}_3)[c(\mathbf{R}_{32}, \mathbf{\Omega}_3, \mathbf{\Omega}_2) + \eta(\mathbf{R}_{32}, \mathbf{\Omega}_3, \mathbf{\Omega}_2)]d\mathbf{R}_3 d\mathbf{\Omega}_3, \quad (1)$$

and the closure

$$c(\mathbf{R}_{12}, \mathbf{\Omega}_1, \mathbf{\Omega}_2) = \exp[-\beta u(\mathbf{R}_{12}, \mathbf{\Omega}_1, \mathbf{\Omega}_2) + \eta(\mathbf{R}_{12}, \mathbf{\Omega}_1, \mathbf{\Omega}_2) + B(\mathbf{R}_{12}, \mathbf{\Omega}_1, \mathbf{\Omega}_2)] - \eta(\mathbf{R}_{12}, \mathbf{\Omega}_1, \mathbf{\Omega}_2) - 1, \quad (2)$$

which yields the direct and indirect correlation functions $c(\mathbf{R}_{12}, \mathbf{\Omega}_1, \mathbf{\Omega}_2)$ and $\eta(\mathbf{R}_{12}, \mathbf{\Omega}_1, \mathbf{\Omega}_2)$, respectively. The bridge function $B(\mathbf{R}_{12}, \mathbf{\Omega}_1, \mathbf{\Omega}_2)$ is neglected in HNC approximation. $\mathbf{R}_{12}$ is the vector, which points from the center of the first molecule to the center of the second one. The orientation of molecule i is represented by a set of Euler angles $\mathbf{\Omega}_i = (\phi_i, \theta_i, \chi_i)$. The necessary inputs are the pair potential $u(\mathbf{R}_{12}, \mathbf{\Omega}_1, \mathbf{\Omega}_2)$, the number density ρ, and temperature T for the Boltzmann factor $\beta = 1/k_B T$. The pair distribution function is obtained from c and η,

$$g(\mathbf{R}_{12}, \mathbf{\Omega}_1, \mathbf{\Omega}_2) = \eta(\mathbf{R}_{12}, \mathbf{\Omega}_1, \mathbf{\Omega}_2) + c(\mathbf{R}_{12}, \mathbf{\Omega}_1, \mathbf{\Omega}_2) + 1. \quad (3)$$

In the MOZ approach, the correlation function as well as the interaction potential are expanded in terms of a basis set of rotational invariants,

$$a(\mathbf{R}_{12}, \mathbf{\Omega}_1, \mathbf{\Omega}_2) = \sum_{mnl} \sum_{\mu\nu} a^{mnl}_{\mu\nu}(R_{12}) \Phi^{mnl}_{\mu\nu}(\boldsymbol{\omega}_R, \mathbf{\Omega}_1, \mathbf{\Omega}_2), \quad (4)$$

where $\boldsymbol{\omega}_R$ denotes the orientation of vector $\mathbf{R}_{12}$. The rotational invariants have the usual definition,

$$\Phi^{mnl}_{\mu\nu}(\boldsymbol{\omega}_R, \mathbf{\Omega}_1, \mathbf{\Omega}_2) = f^{mnl} \sum_{\mu'\nu'\lambda} \begin{pmatrix} m & n & l \\ \mu' & \nu' & \lambda \end{pmatrix} R^m_{\mu'\mu}(\mathbf{\Omega}_1) R^n_{\nu'\nu}(\mathbf{\Omega}_2) R^l_{\lambda 0}(\boldsymbol{\omega}_R), \quad (5)$$

where

$$\begin{pmatrix} m & n & l \\ \mu' & \nu' & \lambda \end{pmatrix}, \quad (6)$$

is a 3j symbol, $R^m_{\mu'\mu}$ is the Wigner generalized rotation matrix,[30] and f^{mnl} is conventionally chosen to be $[(2m+1)(2n+1)]^{1/2}$. The expansion coefficients of the rotation invariants, which characterize the liquid structure, are evaluated as,

$$a^{nl}_{\nu'\nu\lambda}(R_{12}) = \frac{(2n+1)(2l+1)}{32\pi^2} \int\int a(\mathbf{R}_{12}, \mathbf{0}, \mathbf{\Omega}_2) \times R^l_{\lambda 0}(\boldsymbol{\omega}_R)^* R^n_{\nu'\nu}(\mathbf{\Omega}_2)^* d\boldsymbol{\omega}_R d\mathbf{\Omega}_2, \quad (7)$$

$$a^{mnl}_{\mu\nu}(R_{12}) = (2m+1) \sum_{\nu'\lambda} \begin{pmatrix} m & n & l \\ \mu & \nu' & \lambda \end{pmatrix} a^{nl}_{\nu'\nu\lambda}(R_{12}). \quad (8)$$

In performing the integration of Eq. (7), the orientation of molecule 1 is fixed to be zero. The expansion of the MOZ equation (Eq. (1)) in rotation invariants has been described in detail in references.[1,4]

III. METHODS

A. MDIIS algorithm

The residual vector of the iterative subspace is defined as

$$\Delta\eta^{mnl}_{\mu\nu,i}(R_{12}) \equiv \eta^{mnl}_{\mu\nu,i+1}(R_{12}) - \eta^{mnl}_{\mu\nu,i}(R_{12}), \quad (9)$$

where i is the iteration step of the MOZ equation solver. In the DIIS method, the final solution, $\eta^{mnl,*}_{\mu\nu}(R_{12})$ is approximated as a linear combination of previous iteration solution,

$$\eta^{mnl}_{\mu\nu}(R_{12})^\dagger = \sum_{i=1}^{l} c_i \eta^{mnl}_{\mu\nu,i}(R_{12}), \quad (10)$$

where l is the number of previous vectors, and the coefficients c_i are unknown real numbers. The coefficients are required by normalization to add to one,

$$\sum_{i=1}^{l} c_i = 1. \quad (11)$$

The DIIS method also requires the same relation for the residual vectors,

$$\Delta\eta^{mnl}_{\mu\nu}(R_{12})^\dagger = \sum_{i=1}^{l} c_i \Delta\eta^{mnl}_{\mu\nu,i}(R_{12}). \quad (12)$$

From the required conditions of Eqs. (10)–(12), the following algebraic equation is obtained

$$\begin{pmatrix} S_{11} & \cdots & S_{1m} & -1 \\ \vdots & \ddots & \vdots & \vdots \\ S_{m1} & \cdots & S_{mm} & -1 \\ -1 & \cdots & -1 & 0 \end{pmatrix} \begin{pmatrix} c_1 \\ \vdots \\ c_m \\ \lambda \end{pmatrix} = \begin{pmatrix} 0 \\ \vdots \\ 0 \\ -1 \end{pmatrix}, \quad (13)$$

where S_{ij} is the matrix of overlaps, defined on the radial grid of k points,

$$S_{ij} \equiv \left\langle \Delta\eta^{mnl}_{\mu\nu,i}(R_{12}) | \Delta\eta^{mnl}_{\mu\nu,j}(R_{12}) \right\rangle, = \sum_{k=1} \Delta\eta^{mnl}_{\mu\nu,i}(R_k)^* \Delta\eta^{mnl}_{\mu\nu,j}(R_k), \quad (14)$$

and λ is a Lagrangian multiplier. The modification to the DIIS which was proposed by Kovalenko and co-workers[27] updates the basis function as follows,

$$\eta^{mnl}_{\mu\nu}(R_k) = \eta^{mnl}_{\mu\nu}(R_k)^\dagger + \gamma \Delta\eta^{mnl}_{\mu\nu}(R_k)^\dagger, \quad (15)$$

where γ is the mixing parameter to be chosen for the best convergence.

B. Fivefold integration

The discrete version of the fivefold integration in Eq. (7) is expressed with use of the weight for Lebedev-Laikov quadrature, w_i, and the constant weight for Gauss-Chebyshev quadrature, w:

$$a^{nl}_{\nu'\nu\lambda}(R_{12}) = \frac{(2n+1)(2l+1)}{2\pi} \sum_{i=1}^{N}\sum_{j=1}^{N}\sum_{k=1}^{M} \mathrm{w} w_i w_j \times a(R_{12}, \theta_i, \phi_i, \theta_j, \phi_j, \chi_k) d^l_{\lambda 0}(\theta_i) \exp(\lambda\phi_i) \times d^n_{\nu'\nu}(\theta_j) \exp(\nu'\phi_j) \exp(\nu\chi_k), \quad (16)$$

where θ_i and ϕ_i are components of $\boldsymbol{\omega}_R$, and θ_j, in addition ϕ_j, and χ_k are the Euler angles representing the orientation $\boldsymbol{\Omega}_2$. In Eq. (16), $d^n_{\nu'\nu}(\theta_j) = R^n_{\nu'\nu}(0, \theta_j, 0)$. The Lebedev-Laikov quadrature is used for θ_i, ϕ_i, θ_j, and ϕ_j, while the Gauss-Chebyshev quadrature is for χ_k. The parameters N and M are the number of grid points of the Lebedev-Laikov and Gauss-Chebyshev quadratures, respectively. Thanks to the Lebedev-Laikov quadrature, we can replace the five one-dimensional transforms in accelerated method developed by Lado and co-workers[6] to three ones. The numerical integration of the HNC closure is performed for entire space without adopting the linearized HNC closure method proposed by Fries and Patey.[31]

C. Asymptotic behavior of $c^{mnl}_{\mu\nu}$

How to remove the Coulomb tail from direct correlation function in order to get an accurate determination of the corresponding Hankel transform has been an important technical issue for a long time.[17,32–34] For the numerical treatment of the Hankel transform of direct correlation function, the pair potential $u(\mathbf{R}_{12}, \boldsymbol{\Omega}_1, \boldsymbol{\Omega}_2)$ is split into the long-term Coulomb part $u^L(\mathbf{R}_{12}, \boldsymbol{\Omega}_1, \boldsymbol{\Omega}_2)$ and short-term part $u^S(\mathbf{R}_{12}, \boldsymbol{\Omega}_1, \boldsymbol{\Omega}_2)$. Usually, the Gauss error function is used for this splitting,

$$u^L(\mathbf{R}_{12}, \boldsymbol{\Omega}_1, \boldsymbol{\Omega}_2) = \sum_{ij} \frac{q_i q_j}{r_{ij}} \mathrm{erf}(\alpha r_{ij})$$

$$u^S(\mathbf{R}_{12}, \boldsymbol{\Omega}_1, \boldsymbol{\Omega}_2) = u(\mathbf{R}_{12}, \boldsymbol{\Omega}_1, \boldsymbol{\Omega}_2) - u^L(\mathbf{R}_{12}, \boldsymbol{\Omega}_1, \boldsymbol{\Omega}_2), \quad (17)$$

where q_i is partial charge of atom i, r_{ij} is the distance between atoms i and j belonging to different molecules, erf(x) is the error function, and α is a constant appropriately chosen. The rotational invariant coefficients of Eq. (17), $u^{mnl,L}_{\mu\nu}(R_{12})$ are obtained by performing the integration of Eq. (7). The effect of the overlap between molecules which is neglected in the electrostatic multipole expansion is, therefore, included in the coefficients. The Fourier transform of $u^{mnl,L}_{\mu\nu}(R_{12})$ can be found analytically,

$$\tilde{u}^{mnl,L}_{\mu\nu}(k) = \frac{4\pi}{k^2}(2m+1)(2n+1)(2l+1)(-i)^n i^m \times \begin{pmatrix} m & n & l \\ 0 & 0 & 0 \end{pmatrix} \sum_{ij} q_i q_j j_m(k\delta r_i) j_n(k\delta r_j) \times R^m_{\mu 0}(\boldsymbol{\omega}_i) R^n_{\nu 0}(\boldsymbol{\omega}_j) \exp[-k^2/4\alpha^2], \quad (18)$$

where j_n is the nth order spherical Bessel function, δr_i and $\boldsymbol{\omega}_i$ are the radial and angle components of the position of the site i with respect to the center of its molecule. The long-range term part of the direct correlation function, $c^{mnl,L}_{\mu\nu}(R_{12})$ is found using the asymptotic approximation,[35]

$$c^{mnl,L}_{\mu\nu}(R_{12}) \approx -\beta u^{mnl,L}_{\mu\nu}(R_{12}). \quad (19)$$

The short-ranged function, $c^{mnl,S}_{\mu\nu}(R_{12})$ is defined as

$$c^{mnl,S}_{\mu\nu}(R_{12}) = c^{mnl}_{\mu\nu}(R_{12}) - c^{mnl,L}_{\mu\nu}(R_{12}). \quad (20)$$

The forward Hankel transform is adopted to Eq. (20), and $c^{mnl}_{\mu\nu}$ in k-space is obtained by adding Eq. (18) into the transformed function. The exact treatment of the Coulomb interaction developed here makes it possible to apply the "charge up method" which has been used for solving the RISM or three dimensional RISM theories[9] to the MOZ calculation. In the charge up method, the HNC closure is expressed with the parameter λ as follows,

$$g(\mathbf{R}_{12}, \boldsymbol{\Omega}_1, \boldsymbol{\Omega}_2) = \exp[-\beta\{\mathrm{u}^{\mathrm{sr}}(\mathbf{R}_{12}, \boldsymbol{\Omega}_1, \boldsymbol{\Omega}_2) + \lambda u^{\mathrm{el}}(\mathbf{R}_{12}, \boldsymbol{\Omega}_1, \boldsymbol{\Omega}_2)\} + \eta(\mathbf{R}_{12}, \boldsymbol{\Omega}_1, \boldsymbol{\Omega}_2)], \quad (21)$$

where u^{sr} and u^{el} are short range and electrostatic interactions, respectively, and λ is the charge up parameter. Parameter λ increases from zero to one, which is updated after convergence of the MOZ or RISM until $\lambda = 1$. The $c^{mnl,S}_{\mu\nu}$ in Eq. (20) is calculated with use of λ,

$$c^{mnl,S}_{\mu\nu}(R_{12}) = c^{mnl}_{\mu\nu}(R_{12}) - \lambda c^{mnl,L}_{\mu\nu}(R_{12}). \quad (22)$$

The general expression of $c^{mnl,L}_{\mu\nu}$ to all multipole orders is, therefore, required for adopting the charge up method to the MOZ calculation. This method helps one to reduce the iteration steps of the MOZ solution drastically. The adopting of the charge up method was also an important technical issue in extending the RISM to three dimensional RISM (3DRISM) theory.[36] Similarly, the obtained formalism in this section plays a crucial role in applying the MOZ formalism to the three dimensional Cartesian grids approach.

TABLE I. Geometrical and potential parameters for water and ions.

Geometry								
r(OH) [Å]	1.00000							
∠ HOH [deg.]	109.27							
Potential parameters	O	H	Li^+	Na^+	K^+	F^-	Cl^-	Br^-
σ[Å]	3.1660	0.4000	2.1265	3.3304	4.9346	2.7330	4.4172	4.6238
ϵ [kcal/mol]	0.1554	0.0460	0.0183	0.0028	0.0003	0.7200	0.1180	0.0900
Partial charge [e]	− 0.8476	0.4238	1.0000	1.0000	1.0000	− 1.0000	− 1.0000	− 1.0000

IV. RESULTS

A. Bulk water

The MOZ algorithm described previously was applied to the bulk water at density, 0.03334 $Å^{-3}$, and temperature, 300 K. The interaction potential between water molecules is given by

$$u(\mathbf{R}_{12}, \mathbf{\Omega}_1, \mathbf{\Omega}_2) = u^{\mathrm{LJ}}(\mathbf{R}_{12}, \mathbf{\Omega}_1, \mathbf{\Omega}_2) + u^{\mathrm{ES}}(\mathbf{R}_{12}, \mathbf{\Omega}_1, \mathbf{\Omega}_2), \tag{23}$$

$$u^{\mathrm{LJ}}(\mathbf{R}_{12}, \mathbf{\Omega}_1, \mathbf{\Omega}_2) = 4\sum_{ij} \epsilon_{ij} \left\{ \left(\frac{\sigma_{ij}}{r_{ij}}\right)^{12} - \left(\frac{\sigma_{ij}}{r_{ij}}\right)^{6} \right\}, \tag{24}$$

$$u^{\mathrm{ES}}(\mathbf{R}_{12}, \mathbf{\Omega}_1, \mathbf{\Omega}_2) = \sum_{ij} \frac{q_i q_j}{r_{ij}}, \tag{25}$$

where ϵ_{ij} and σ_{ij} are the usual Lennard-Jones parameters. In this article, we apply Lorentz-Berthlot combine rule to these LJ parameters. The molecular parameters associated with solvent water are summarized in Table I. The rotational invariant expansion was truncated for $m \le m_{\max}$ and $n \le m_{\max}$ with $m_{\max} = 4$. In all numerical calculations, the number of grid points for the radial length was chosen to be 512 with a spacing $dr = 0.07$ Å.

The dielectric constant ϵ is calculated from the following Kirkwood formula,

$$\frac{(\epsilon - 1)(2\epsilon + 2)}{9\epsilon} = y_D g_{\mathrm{K}}, \tag{26}$$

where g_{K} is the Kirkwood factor and $y_D = 4\pi\rho\mu^2/9k_{\mathrm{B}}T$ with μ being the dipole moment. The R-dependent Kirkwood factor G_{K} is defined as

$$G_{\mathrm{K}}(R) = 1 - \frac{4\pi\rho}{\sqrt{3}} \int_0^R g_{00}^{110}(R_{12}) R_{12}^2 dR_{12}. \tag{27}$$

According to Eq. (26), it tends to the usual Kirkwood factor, $\lim_{R\to\infty} G_{\mathrm{K}}(R) = g_{\mathrm{K}}$, which is used to calculate the dielectric constant.

The lowest order pair correlation function g_{00}^{000}, the radial distribution functions, and the $G_{\mathrm{K}}(R)$ obtained from the solvent-solvent MOZ equation are shown in Figures 1(a) and 1(b), respectively. The results of 38, 50, and 86 Lebedev-Laikov grids are also shown in Figure 1. As one can see, there is no difference in g_{00}^{000} between all grids. In contrast, $G_{\mathrm{K}}(R)$ for 38 grid points at long distance is slightly lower than those for another grid points. If we look at Table II, we see that this difference has an influence on the resulting dielectric constant. g_{00}^{110} which is responsible for the behavior of G_{K} is shown in Figure 1(c). It has a distinct negative peak at $R \sim 2.8$Å. The negative peaks for the Lebedev-Laikov grids are summarized in Table II. The minimum for 38 grid points is slightly higher than those for another cases. This indicates that the resulting dielectric constant is sensitive to the small difference of g_{00}^{110}. Consequently, it can be concluded that the appropriate Lebedev-Laikov grid for the convergent calculation of water requires at least 50 grid points. Note that the calculated dielectric constant is smaller than the experimental result, 78.9. Since the dipole moment of water also contributes to its dielectric property, the quantitative improvements require not only for the accurate calculation of the pair correlation function but also the sophisticated model of water. Recent development done by Yoshida and Kato[7] could improve the dielectric constant by taking the electronic structure of water into the MOZ calculation. In Figure 1(d), g_{00}^{112} for the grids are compared. Since there is no clear difference in g_{00}^{112} between 50 and 86 grid points, 50 grid points is accurate enough for the further discussion of higher order correlation functions.

The iteration steps to achieve the convergence of the MOZ calculations of bulk water at $T = 3000$ K with different methods are compared in Figure 2. The iterations are finished

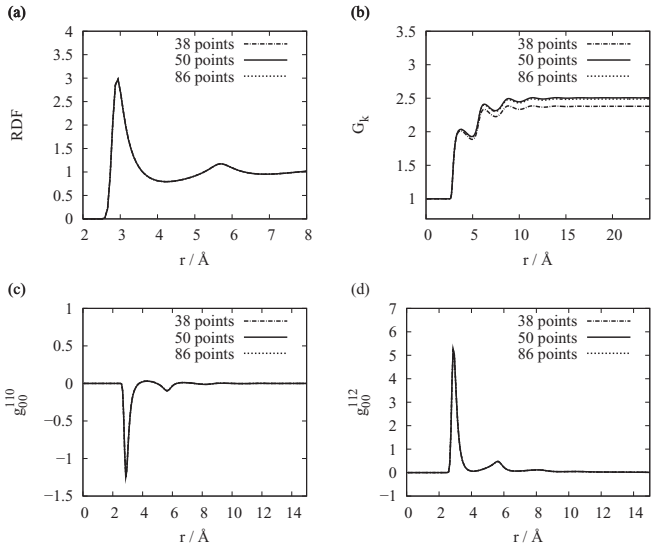

FIG. 1. The pair correlation functions for ambient water. (a) The radial distribution function g_{00}^{000}. (b) R-dependent Kirkwood factor. (c) g_{00}^{110}. (d) g_{00}^{112}. The dashed-bar, solid, and dotted lines are the results of the 38, 50, and 86 Lebedev-Laikov grids, respectively.

TABLE II. Grid dependency of the dielectric constant and negative peaks of g_{00}^{110} at $r \sim 2.8$ Å for the Lebedev-Laikov quadrature.

Number of grids	ϵ	Peak
38	63.0604	−1.2072
50	66.3859	−1.2490
74	66.3878	−1.2463
86	65.9105	−1.2431
110	66.1803	−1.2404

once

$$\sum_J |\eta_J^{\mathrm{New}} - \eta_J^{\mathrm{Old}}|/N_J < 1.0^{-9} \tag{28}$$

is satisfied. Here, η_J denote all the iteration variables in the methods, superscripts "New" and "Old" represent the old and new values, respectively, and N_J is the total number of the variables. Following our previous results, we used 50 grid points of the Lebedev-Laikov grids for the fivefold integrals. As is evident from this figure, the MDIIS method is effective for reducing the iteration steps to achieve the convergence of the MOZ calculation. This remarkable convergence property is characteristic for our efficient algorithm, especially for the charge up method. Now, we also calculated the MOZ with use of the hybrid algorithm of the NR with the Picard method developed by Kinoshita and Harada.[16] It took more than 30 000 iteration steps to obtain the result of ambient water because it was needed to be started from 1000 K in order to avoid divergence. In contrast, our efficient algorithm which was started from 300 K could converge under 800 steps.

B. Aqueous ions in solution

Here, we apply the MOZ equation to the excess chemical potential of an aqueous ion in solution. The same solvent system with the preceding subsection is employed. The optimized potentials for liquid simulations parameters[37] used for the Lennard-Jones parameters of ions are summarized in Table I. From the previous analysis of ambient water, we used 50 grid points for the Lebedev-Laikov quadrature. The radial distribution functions between ions and water are shown in Figures 3(a) and 3(b). We can see that the first peaks for lithium, sodium, and fluoride ions are higher and narrower

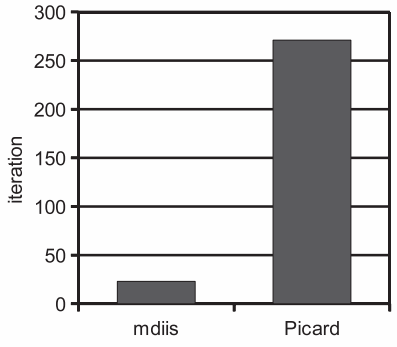

FIG. 2. Comparison of the iteration step of the MOZ calculation with the Picard methods.

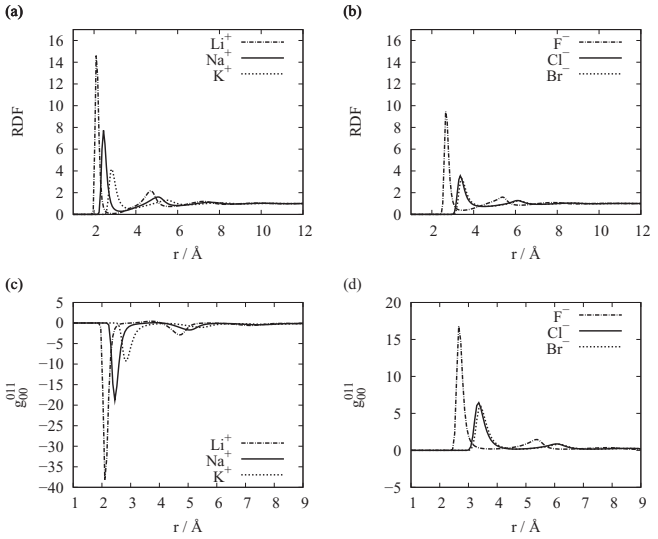

FIG. 3. The pair correlation functions between an ion and water. (a) The radial distribution function g_{00}^{000} between cations and water: The dashed-bar, solid, and dotted lines are results of lithium, sodium, and potassium ions, respectively. (b) g_{00}^{000} between anions and water. (c) g_{00}^{011} between cations and water. (d) g_{00}^{011} between anions and water. The dashed-bar, solid, and dotted lines are results of fluoride, chloride, and bromide ions, respectively.

than those for another ions, indicating a strong binding of water molecules to these ions. On the other hand, the wide broaden peaks for potassium, chloride, and bromide ions mean the thermal fluctuation of their hydration structure. Figures 3(c) and 3(d) show the real part of g_{00}^{011} representing the probability distribution of the dipole moment of water around cations and anions, respectively. The broaden major peaks found in g_{00}^{011} for potassium, chloride, and bromide ions are result of the thermal fluctuation of the direction of water dipole at first hydration shell. In contrast, the dipole around another ions has a specific direction due to the size effect of ions. These findings are consistent with the well-established models of hydration for relatively large ions, that is, the negative hydration or the structure breaking effect.[38,39]

The excess chemical potential $\Delta\mu^{\mathrm{ex}}$ for HNC approximation is represented as follows,[15]

$$\Delta\mu^{\mathrm{ex,MOZ}} = 4\pi\rho k_{\mathrm{B}}T \int_0^\infty \left[\frac{1}{2}\eta_{00}^{000}(R_{12})h_{00}^{000}(R_{12}) - c_{00}^{000}(R_{12})\right] \times R_{12}^2 dR_{12}. \tag{29}$$

We also compared $\Delta\mu^{\mathrm{ex,\,MOZ}}$ with one for the RISM theory. Theoretical and numerical details are summarized in the book of Hirata.[9] The analytical expression of the $\Delta\mu^{\mathrm{ex,\,RISM}}$ for the RISM-HNC approximation is similarly represented as follows,[40]

$$\Delta\mu^{\mathrm{ex,RISM}} = 4\pi\rho k_{\mathrm{B}}T \sum_{\alpha\beta} \int_0^\infty \left[\frac{1}{2}\eta_{\alpha\beta}(r)h_{\alpha\beta}(r) - c_{\alpha\beta}(r)\right] r^2 dr, \tag{30}$$

where α and β are the atomic sites belonging to different molecules, and r is the intermolecular separation between sites α and β. The meaning of function $h_{\alpha\beta}$, $c_{\alpha\beta}$, and $\eta_{\alpha\beta}$ are the natural extension of those for the MOZ formalism to the

TABLE III. Excess chemical potential, $\Delta\mu^{ex}$, calculated from the MOZ and RISM theory.

Ion	$\Delta\mu^{ex}$ (MOZ) [kcal/mol]	$\Delta\mu^{ex}$ (RISM) [kcal/mol]
Li^+	− 24.7694	− 97.4281
Na^+	− 15.1301	− 76.3796
K^+	− 7.4864	− 57.3009
F^-	− 9.5618	− 131.4526
Cl^-	3.4937	− 75.5790
Br^-	4.8474	− 71.2814

interaction site model. For the RISM calculation, the number of grid points for r was chosen to be 1024 with the width of 0.05 Å.

In Table III, we show the excess chemical potentials $\Delta\mu^{ex}$ calculated from the MOZ and RISM theory. Both methods show the increasing of the $\Delta\mu^{ex}$ in proportion as the ionic radius increase. Surprisingly, the MOZ theory shows the irrelevant positive values of the excess chemical potentials for chloride and bromide ions. On the other hand, the RISM theory can predict the negative values for all ions. Since the hydration structure around an anion is characterized by the H-bond network of water molecules, it is essential to include the multi-body correlation functions into the excess chemical potentials. Similarly, it has been pointed out that the thermodynamics of molecular liquids with the MOZ-HNC theory are smaller than the molecular dynamics (MD) results.[41] These differences, therefore, indicate that the RISM-HNC theory can extract some higher order correlations neglected in the MOZ-HNC theory by employing the site-site approximation. The obtained results in this article encourage the MOZ theory to be coupled with the site-site approximation for the effective bridge functions.

V. CONCLUSIONS

In this article, we adopted the MDIIS and the charge up method for solving the MOZ equation. Compared to the previous algorithms such as the Newton-Raphson method, these methods allow us to obtain the MOZ results within a few iteration steps. In averaging the correlation functions over orientations, we used the Gauss-Legendre and Lebedev-Laikov quadrature. The latter quadrature is effective for reducing the computational cost for calculating the fivefold integration of the closure approximation. To show the effectiveness of our method, we performed numerical investigations for the ambient water and ions in aqueous solutions. In the study of bulk water, we decided the appropriate Lebedev-Laikov grid for accurate calculation of the higher order correlation functions which is responsible for the dielectric properties of liquids. Although the grid dependencies were not found in the radial distribution functions, it was shown that the R-dependent Kirkwood factor requires at least 50 grid points. To investigate the contribution of the neglected correlation functions in the RISM formalism, we calculated the excess chemical potential for aqueous ions with the MOZ- and RISM-HNC theory. The results indicate that both theories show the decreasing of excess chemical potential in proportion as the ion sizes increase. The results of the MOZ-HNC theory show the irrelevant positive values of the excess chemical potentials for chrome and bromide ions. In contrast, the RISM-HNC theory can predict the negative values for all ions. Although the physical interpretation of these differences is not clear, the site-site representation of the HNC closure is effective for the thermodynamics of solvated ions. Our analysis of aqueous ions indicates that the difference between the MOZ-HNC and RISM-HNC theories is an important key to studying the higher order correlation functions neglected in the HNC approximation.

ACKNOWLEDGMENTS

Authors are supported by Grant-in-Aid for Young Scientists (B) from Japan Society for the Promotion of Science (JSPS) and Grant-in-Aid for Scientific Research on Innovative Areas (20107008, 23118719) from the Ministry of Education, Culture, Sports, Science and Technology (MEXT) in Japan. We thank Professor B. Montgomery. Pettitt for stimulating discussions.

[1] L. Blum and A. J. Torruella, J. Chem. Phys. **56**, 303 (1972).
[2] L. Blum, J. Chem. Phys. **57**, 1862 (1972).
[3] L. Blum, J. Chem. Phys. **58**, 3295 (1973).
[4] P. G. Kusalik and G. N. Patey, Mol. Phys. **65**, 1105 (1988).
[5] P. G. Kusalik and G. N. Patey, J. Chem. Phys. **88**, 7715 (1988).
[6] F. Lado, E. Lomba, and M. Lombardero, J. Chem. Phys. **103**, 481 (1995).
[7] N. Yoshida and S. Kato, J. Chem. Phys. **113**, 4974 (2000).
[8] D. Chandler and H. C. Andersen, J. Chem. Phys. **57**, 1930 (1972).
[9] *Molecular Theory of Solvation*, edited by F. Hirata, (Kluwer Academic, Dordrecht, 2003).
[10] B. M. Pettitt and P. J. Rossky, J. Chem. Phys. **77**, 1452 (1982).
[11] J. S. Hoye and G. Stell, J. Chem. Phys. **65**, 18 (1976).
[12] J. Perkyns and B. M. Pettitt, J. Chem. Phys. **97**, 7656 (1992).
[13] D. Chandler, R. Silbey, and B. M. Ladanyi, Mol. Phys. **46**, 1335 (1982).
[14] D. Chandler, C. G. Joslin, and J. M. Deutch, Mol. Phys. **47**, 871 (1982).
[15] C. G. Gray and C. G. Gubbins, *Theory of Molecular Fluids*, (Oxford University Press, Belfast, 1984), Vol. I.
[16] M. Kinoshita and M. Harada, Mol. Phys. **65**, 599 (1988).
[17] K. Ng, J. Chem. Phys. **61**, 2680 (1974).
[18] P. A. Monson and G. P. Morriss, Adv. Chem. Phys. **77**, 451 (1990).
[19] M. J. Gillan, Mol. Phys. **38**, 1781 (1979).
[20] S. Labik, A. Malijevsky, and P. Vonka, Mol. Phys. **56**, 709 (1985).
[21] S. Woelki, H. H. Kohler, H. Krienke, and G. Schmeer, Phys. Chem. Chem. Phys. **10**, 898 (2008).
[22] G. N. Chuev and M. V. Fedorov, J. Comput. Chem. **25**, 1369 (2004).
[23] G. N. Chuev and M. V. Fedorov, J. Chem. Phys. **120**, 1191 (2004).
[24] M. V. Fedorov and G. N. Chuev, J. Mol. Liq. **120**, 159 (2005).
[25] P. Pulay, Chem. Phys. Lett. **73**, 393 (1980).
[26] P. Pulay, J. Comput. Chem. **3**, 556 (1982).
[27] A. Kovalenko, S. Ten-no, and F. Hirata, J. Comput. Chem. **20**, 928 (1999).
[28] V. I. Lebedev and D. N. Laikov, Russ. Acad. Sci. Dokl. Math. **59**, 477 (1999).
[29] S. L. Carnie, D. Y. C. Chan, and G. R. Walker, Mol. Phys. **43**, 1115 (1981).
[30] A. Messiah, *Quantum Mechanics* (Wiley, New York, 1962).
[31] P. H. Fries and G. N. Patey, J. Chem. Phys. **82**, 429 (1985).
[32] F. Lado, Mol. Phys. **31**, 1117 (1976).
[33] A. R. Allnatt, Mol. Phys. **8**, 533 (1964).
[34] X. S. Chen and F. Forstmann, Condens. Matter Phys. **4**, 679 (2001).
[35] J. L. Lebowitz and J. K. Percus, Phys. Rev. **144**, 251 (1966).
[36] J. Perkyns, G. C. Lynch, J. J. Howard, and B. M. Pettitt, J. Chem. Phys. **132**, 064106 (2010).
[37] W. L. Jorgensen and N. A. McDonald, J. Mol. Struct.: THEOCHEM **424**, 145 (1998).
[38] H. S. Frank and W. Y. Wen, Discuss. Faraday. Soc. **44**, 133 (1957).
[39] O. Y. Samoilov, Discuss. Faraday. Soc. **44**, 141 (1957).
[40] S. J. Singer and D. Chandler, Mol. Phys. **55**, 621 (1985).
[41] J. Richardi, C. Millot, and P. H. Fries, J. Chem. Phys. **110**, 1138 (1999).